Heating and evaporation of a two-component droplet: hydrodynamic and kinetic models

Sazhin, S. S. , Shishkova, I. N. and Al Qubeissi, M.

Original citation & hyperlink:
Sazhin, S. S. , Shishkova, I. N. and Al Qubeissi, M. (2014) Heating and evaporation of a two-component droplet: hydrodynamic and kinetic models. International Journal of Heat and Mass Transfer, volume 79 : 704-712
http://dx.doi.org/10.1016/j.ijheatmasstransfer.2014.08.026

ISSN 0735-1933
DOI 10.1016/j.ijheatmasstransfer.2014.08.026

http://curve.coventry.ac.uk/open

Heating and evaporation of a two-component droplet: hydrodynamic and kinetic models

S.S. Sazhin[1*], I.N. Shishkova[2,1], M. Al Qubeissi[1]

[1] *Sir Harry Ricardo Laboratories, Centre for Automotive Engineering, School of Computing, Engineering and Mathematics, Faculty of Science and Engineering, University of Brighton, Brighton, BN2 4GJ, UK*

[2] *Low Temperature Department, Moscow Power Engineering Institute, Krasnokazarmennaya 14, Moscow 111250, Russia*

Abstract

A previously developed kinetic model for two-component vapour and background gas (air) is applied to the analysis of droplet heating and evaporation in Diesel engine-like conditions. The model used in the analysis is based on the introduction of the kinetic region in the immediate vicinity of the droplets and the hydrodynamic region. The presence of two components in the vapour, finite thermal conductivity and finite species diffusivity in droplets are taken into account. It is pointed out that for parameters which are typical of Diesel engine-like conditions, the heat flux in the kinetic region is a linear function of the temperature at the outer boundary of this region, but is almost independent of the density of the components at this boundary. Mass fluxes of both components in the kinetic region are shown to decrease almost linearly with increasing vapour density at the outer boundary of this region, but are almost independent of the temperature drop in the kinetic region. The model is tested for the analysis of heating and evaporation of a droplet with initial radius and temperature equal to 5 μm and 300 K, respectively, immersed into gas with temperatures 1000 K and 700 K for several mixtures of n-dodecane and p-dipropylbenzene. It is pointed out that an increase in the mass fraction of p-dipropylbenzene and kinetic effects lead to an increase in the predicted droplet evaporation time. The kinetic effects

*Corresponding author. Tel. +44(0)1273642677; fax +44(0)1273642330; e-mail S.Sazhin@brighton.ac.uk

are shown to increase with increasing gas temperature and molar fraction of p-dipropylbenzene.

Keywords:
Boltzmann equation, Diesel fuel droplet, n-dodecane, p-dipropylbenzene, heat/mass transfer, mixture

---

Nomenclature

B_M	Spalding mass transfer number
B_T	Spalding heat transfer number
c	specific heat capacity
D	binary diffusion coefficient
f	molecular velocity distribution function
E	relative error defined by Equation (18)
h	convection heat transfer coefficient
j	mass flux
J	collision integral
k	thermal conductivity
ℓ	mean free path
L	latent heat of evaporation
Le	Lewis number
m	mass
M	molar mass
N_{at}	the total number of atoms in a molecule
Nu	Nusselt number
p	pressure
Pr	Prandtl number
q	heat flux
Q_L	power spent on droplet heating
$\mathbf{r}$	radius-vector
R	distance from the centre of the droplet
$R_{v(a)}$	gas constant referring to n-dodecane (air)
R_d	droplet radius
Sc	Schmidt number
T	temperature
$\mathbf{v}$	velocity
X	molar fraction

Y	mass fraction

Greek symbols

α	parameter defined by Equation (6)
β	evaporation coefficient
δ_{Rd}	thickness of the kinetic region
ϵ_i	evaporation rate of individual species
θ	angular coordinate
κ	liquid diffusivity
ρ	density
σ	effective diameter of molecules
ϕ	angular coordinate

Subscripts

a	air
at	atom
α, β	$\alpha = a, n, p$; $\beta = a, n, p$
d	droplet
eff	effective
g	gas
h	hydrodynamic
i	components
k	kinetic
l	liquid
n	n-dodecane
p	constant pressure or p-dipropylbenzene
r	reference or reflected
Rd	outer boundary of the kinetic region
s	surface
total	total
v	fuel vapour
0	initial
∞	ambient

Superscripts

i	components
$\prime$	after the collision
$\sim$	normalised

1. Introduction

An interest in modelling droplet heating and evaporation has been stimulated by various engineering, environmental and pharmaceutical applications [1, 2]. In most engineering applications, including automotive ones, the modelling of these processes has been based on the hydrodynamic approximation, although the limitations of this approximation, even in the case when these processes take place at high pressures, are well known (see [3, 4, 5]). In a number of studies, including [6]-[9], the evaporation of n-dodecane $C_{12}H_{26}$ (an approximation for Diesel fuel) was studied and a new model was developed based on a combination of the kinetic and hydrodynamic approaches. In the immediate vicinity of droplet surfaces (up to about one hundred molecular mean free paths), the vapour and ambient gas dynamics were studied based on the Boltzmann equation (kinetic region), while at larger distances the analysis was based on the hydrodynamic equations (hydrodynamic region). Mass, momentum and energy fluxes were conserved at the interface between these regions. The authors of [7, 8, 9] considered the problem of n-dodecane evaporation into air and developed a new numerical algorithm for the solution of a system of two Boltzmann equations for n-dodecane and air, taking into account elastic collisions between: n-dodecane molecules; between air molecules; and between n-dodecane and air molecules. A new approach to taking into account the effects of inelastic collisions was developed in [10] and applied to the problem of n-dodecane droplet heating and evaporation in [11].

One of the important limitations of the approaches described in [6]-[11] is that they were based on the assumption that Diesel fuel can be approximated by n-dodecane. A more detailed analysis of the composition of Diesel fuel showed that it includes hundreds of various hydrocarbon components [12, 13, 14]. It is obviously not possible to take into account the contributions of all these components in the kinetic modelling. At the same time, one can see that these components can be subdivided into two main groups: alkanes and aromatics [14]. The assumption that n-dodecane can approximate alkanes is widely used (see [12, 15, 16]), while aromatics could be approximated by p-dipropylbenzene [15]. In this case it was suggested that a more accurate approximation of Diesel fuel, compared with the one based on

its approximation by n-dodecane, could be its approximation by a mixture of n-dodecane and p-dipropylbenzene. Mass fractions of n-dodecane in this mixture could vary from 0.8 to 0.7 [15, 12].

A new kinetic algorithm for modelling of a three component (two components, approximating Diesel fuel, and air, approximated by nitrogen) mixture was developed in [17]. Binary collisions between molecules were taken into account assuming that these collisions are elastic or inelastic. The functionality testing of the algorithm was performed using a simple test problem of heat and mass transfer in a mixture of n-dodecane, p-dipropylbenzene and nitrogen between two infinite parallel walls. It was concluded that the predictions of the new kinetic algorithm are qualitatively consistent with the predictions of more basic models of the phenomena for which it was tested.

The aim of this paper is to investigate the kinetic effects on heating and evaporation of two-component droplets, approximating Diesel fuel, assuming that this approximation is a mixture of n-dodecane and p-dipropylbenzene. The numerical algorithm developed in [17] will be used in our analysis.

The mathematical model, used in the analysis, is discussed in Section 2. In Section 3 this model is applied to the analysis of heating and evaporation of a two-component (mixture of n-dodecane and p-dipropylbenzene) droplet. The results are compared with those based on the approximation of Diesel fuel droplets by n-dodecane droplets. The main results of the paper are summarised in Section 4.

2. Mathematical models

As in [6]-[11], two regions above the surface of an evaporating fuel droplet are considered: the kinetic and hydrodynamic regions. As in [11], we take into account that thermal conductivity of the liquid phase is finite, and identify the third region called the liquid phase region. All three regions are schematically shown in Fig. 1. T_s and $\rho_{s\,(n,p)}$ refer to the surface temperature and vapour density (for n-dodecane (n) and p-dipropylbenzene (p)) in the immediate vicinity of the droplet surface; T_{Rd} and $\rho_{Rd\,(n,p)}$ refer to the same parameters but at the interface between the kinetic and the hydrodynamic regions. δ_{Rd} is the thickness of the kinetic region. In contrast to [11], we take into account the diffusion of species in the liquid phase and the presence of up to 3 components in the kinetic region. The conventional hydrodynamic analysis is applied in the liquid and hydrodynamic regions, while vapour and air dynamics in the kinetic region are described by the Boltzmann equations.

The hydrodynamic and kinetic models used in our analysis are described below.

2.1. Hydrodynamic model

The hydrodynamic model for the liquid and gas phases, used in our analysis, is essentially the same as described in [14]. In what follows the most essential features of this model are briefly summarised.

A droplet is assumed to be spherical, stationary (the generalisation of the model to a moving droplet is described in [14]) and the process of its heating is described by the following transient heat conduction equation for the temperature $T \equiv T(t, R)$ in the liquid phase:

$$\frac{\partial T}{\partial t} = \kappa \left(\frac{\partial^2 T}{\partial R^2} + \frac{2}{R} \frac{\partial T}{\partial R} \right), \tag{1}$$

where $\kappa = k_l/(c_l \rho_l)$ is the liquid thermal diffusivity, k_l, c_l, and ρ_l are the liquid thermal conductivity, specific heat capacity, and density respectively, R is the distance from the centre of the droplet, t is time.

Equation (1) is to be solved for $0 \leq R < R_d$, where R_d is the droplet radius, with the following initial condition $T(t = 0) = T_{d0}(R)$ and the boundary condition (assuming that the effects of evaporation can be ignored):

$$q_s \equiv h(T_g - T_s) = k_l \left. \frac{\partial T}{\partial R} \right|_{R=R_d-0}, \tag{2}$$

where $T_s = T_s(t)$ is the droplet's surface temperature, $T_g = T_g(t)$ is the ambient gas temperature, h is the convection heat transfer coefficient, linked with the Nusselt number Nu via the equation $\mathrm{Nu} = 2R_d h/k_g$, k_g is the gas thermal conductivity. We assume that fuel vapour is dilute and k_g is equal to the thermal conductivity of ambient air. Remembering the physical background to the problem, we are interested only in the solution which is continuously differentiable twice in the whole domain. This implies that T should be bounded for $0 \leq R < R_d$.

Our analysis is based on the analytical solution to Equation (1), subject to the above-mentioned boundary and initial conditions, which was implemented into a numerical code [14]. To take into account the effect of droplet evaporation in the analytical solution, gas temperature was replaced with the effective temperature defined as: $T_{\text{eff}} = T_g + \frac{\rho_l L \dot{R}_d}{h}$, where L is the latent heat of evaporation, the value of $\dot{R}_d$ is taken from the previous time step and

estimated based on Equation (8). R_d is assumed constant in the analytical solutions, but is updated at the end of the time step Δt to take into account the effects of swelling and evaporation (the effects of non-constant R_d during the time step are discussed in our previous papers, the results of which are summarised in [5]). The value of Nu is estimated as:

$$\mathrm{Nu} = 2\frac{\ln(1+B_T)}{B_T}, \tag{3}$$

where $B_T = \frac{c_{pv}(T_g - T_s)}{L_{\mathrm{eff}}}$ is the Spalding heat transfer number, $L_{\mathrm{eff}} = L + \frac{Q_L}{\dot{m}_d} = \sum_i \epsilon_i L_i + \frac{Q_L}{\sum_i \dot{m}_i}$, Q_L is the power spent on droplet heating, c_{pv} is the specific heat capacity of fuel vapour (estimated for the mixture of vapour species), $\epsilon_i = \epsilon_i(t)$ are the evaporation rates of species i, $\dot{m}_i = \epsilon_i \dot{m}_d$, $\dot{m}_d$ is the droplet evaporation rate (see Equation (8); $\dot{m}_d = \sum_i \dot{m}_i$). $i = n, p$ in our analysis, where n refers to n-dodecane while p refers to p-dipropylbenzene.

Equations for mass fractions of liquid species $Y_{li} \equiv Y_{li}(t, R)$ are presented in the following form:

$$\frac{\partial Y_{li}}{\partial t} = D_l \left(\frac{\partial^2 Y_{li}}{\partial R^2} + \frac{2}{R}\frac{\partial Y_{li}}{\partial R} \right), \tag{4}$$

where D_l is the liquid diffusivity, assumed to be the same for all species and all species concentrations.

Equation (4) was solved analytically with the following boundary condition:

$$\alpha(\epsilon_i - Y_{lis}) = -D_l \left. \frac{\partial Y_{li}}{\partial R} \right|_{R=R_d-0}, \tag{5}$$

and the initial condition $Y_{li}(t=0) = Y_{li0}(R)$, where $Y_{lis} = Y_{lis}(t)$ are liquid components' mass fractions at the droplet's surface,

$$\alpha = \frac{|\dot{m}_d|}{4\pi\rho_l R_d^2}. \tag{6}$$

Assuming that species concentrations in the ambient gas are equal to zero, the values of ϵ_i were found from the following relationship:

$$\epsilon_i = \frac{Y_{vis}}{\sum_{i=n,p} Y_{vis}}, \tag{7}$$

where the subscript $_v$ indicates the vapour phase. The condition $\alpha = \text{const}$ can always be guaranteed for sufficiently small time steps.

The Wilke-Chang approximation was used for the estimate of D_l assuming that the average Lennard-Jones length of molecules is equal to that of n-dodecane (7.12 Å; see Table 1).

The droplet's evaporation rate is estimated from the following equation:

$$\dot{m}_d = -4\pi R_d D_v \rho_{\text{total}} \ln(1 + B_M), \tag{8}$$

where D_v is the binary diffusion coefficient of vapour in air, B_M is the Spalding mass transfer number defined as:

$$B_M = \frac{\rho_{vs} - \rho_{v\infty}}{\rho_{gs}} = \frac{Y_{vs} - Y_{v\infty}}{1 - Y_{vs}}, \tag{9}$$

Y_v is the vapour mass fraction. B_T and B_M are linked by the equation $B_T = (1 + B_M)^{\varphi} - 1$, where $\varphi = \left(\frac{c_{pv}}{c_{pa}}\right) \frac{1}{\text{Le}}$, $\text{Le} = k_g/(c_{pa}\rho_{\text{total}} D_v) = \text{Sc}_d/\text{Pr}_d$ is the Lewis number; it was assumed that $Y_{v\infty} = 0$. Note that the derivation of Equation (8) is essentially based on the assumption that ρ_{total} remains the same at all distances from the droplet surface.

We assume that Diesel fuel vapour diffuses from the surface of the droplet, without changing its composition, with the average diffusion coefficient assumed to be equal to that of n-dodecane in air [18]

$$D_v = 5.27 \times 10^{-6} \left(\frac{T}{300}\right)^{1.583} p^{-1}, \tag{10}$$

where D_v is in m^2/s, T is temperature in K, p is in bar. Note that there is a typo in Eq. (39) in [14]; this typo does not affect the results of the paper as the correct formula was used in the numerical code.

All liquid properties are calculated for the average temperature inside droplets. All gas properties are calculated for the reference temperature $T_r = (2/3)T_s + (1/3)T_g$, where T_s and T_g are droplet surface and ambient gas temperatures, respectively. Enthalpy of evaporation and saturated vapour pressure are estimated at the surface temperature T_s.

The mixtures are treated as ideal (Raoult's law is assumed to be valid). In this case, partial pressures of individual components are estimated as:

$$p_{vi} = X_{lsi}\, p^{\text{sat(i)}}, \tag{11}$$

where X_{lsi} are the molar fractions of liquid components at the surface of the droplet, $p^{\mathrm{sat(i)}}$ are saturated vapour pressures of the ith component ($i = n,\ p$) assuming that this is the only component present in the droplet.

The following approximations for $p^{\mathrm{sat(i)}}$ are used in our analysis:

$$p^{\mathrm{sat(n)}} = \exp\left[8.1948 - 7.8099\,(300/T_s) - 9.0098\,(300/T_s)^2\right] \quad \text{bar} \tag{12}$$

for n-dodecane, and

$$\log_{10}\left[0.001 \times p^{\mathrm{sat(p)}}(n)\right] = A(n) - \frac{B(n)}{T + C(n)}, \tag{13}$$

where

$$A(n) = 0.0007\ n^2 - 0.0064\ n + 6.0715,$$
$$B(n) = 51.811\ n + 1049.1,$$
$$C(n) = 0.1215\ n^2 - 9.6892\ n + 11.161,$$

for p-dipropylbenzene. Pressure in Formula (13) is in Pa.

Note that none of the above expressions for $p^{\mathrm{sat(i)}}$ can be considered reliable at temperatures close to or above critical temperatures. Heating of the droplets above these temperatures, sometimes predicted by the model at the very final stage of droplet evaporation, does not describe accurately the physical background of the processes at this stage. The contribution of the processes at this stage of droplet heating and evaporation to the overall droplet heating and evaporation, however, is expected to be small. To mitigate this behaviour of droplet surface temperature, pressures predicted by Formula (12) and (13) were artificially increased when the temperatures exceeded the corresponding critical temperatures. This affected the very final stage of droplet evaporation (when their mass becomes less than about 1% of the initial mass) and produced negligible effects on the overall process of heating and evaporation.

The mass flux of components evaporating from the droplet surface is estimated as:

$$j_{vi} = \frac{\epsilon_i\,|\dot{m}_d|}{4\pi R_d^2}. \tag{14}$$

2.2. Kinetic model

The kinetic model for a three component mixture, described in [17], is used in our analysis. We consider a mixture of air (approximated by nitrogen), n-dodecane and p-dipropylbenzene (exactly the same analysis is applicable to any other mixture). The evolution of the molecular velocity distribution functions of these three components, $f_a \equiv f_a(\mathbf{r}, t, \mathbf{v})$, $f_n \equiv f_n(\mathbf{r}, t, \mathbf{v})$ $f_p \equiv f_p(\mathbf{r}, t, \mathbf{v})$, is controlled by the following system of Boltzmann equations:

$$\left.\begin{array}{l} \frac{\partial f_a}{\partial t} + \mathbf{v}_a \frac{\partial f_a}{\partial \mathbf{r}} = J_{aa} + J_{an} + J_{ap} \\ \frac{\partial f_n}{\partial t} + \mathbf{v}_n \frac{\partial f_n}{\partial \mathbf{r}} = J_{na} + J_{nn} + J_{np} \\ \frac{\partial f_p}{\partial t} + \mathbf{v}_p \frac{\partial f_p}{\partial \mathbf{r}} = J_{pa} + J_{pn} + J_{pp} \end{array}\right\}, \tag{15}$$

where $J_{\alpha\beta}$ ($\alpha = a, n, p;\ \beta = a, n, p$) are collision integrals, taking into account the contribution of the collisions between molecules; the following explicit expressions for the collision integrals $J_{\alpha\beta}$ are used [7]:

$$J_{\alpha\beta} = \frac{\sigma_{\alpha\beta}^2}{2} \int_{-\infty}^{+\infty} \mathrm{d}\mathbf{v_1} \int_0^{\pi} \sin\theta \mathrm{d}\theta \int_0^{2\pi} \mathrm{d}\phi \left(f_\alpha^{'} f_{\beta 1}^{'} - f_\alpha f_{\beta 1} \right) \left| \mathbf{v}_\alpha - \mathbf{v}_{\beta 1} \right|, \tag{16}$$

where $\sigma_{\alpha\beta} = (\sigma_\alpha + \sigma_\beta)/2$, σ_α and σ_β are the corresponding effective diameters of molecules of air 'a', n-dodecane 'n' and p-dipropylbenzene 'p', θ and ϕ are angular coordinates of molecules β relative to molecules α, superscript $^{'}$ indicates the velocities and the distribution functions after collisions, subscript $_1$ indicates that the function f_α is modified under the influence of collisions with molecules of the type $_\beta$. The first integral on the right hand side of (16) is calculated in the three dimensional velocity space. Expression (16) is the same as that used in [7], where the contribution of only 2 components in the kinetic region was taken into account. This is justified by the fact that triple collisions are ignored.

All collision integrals $J_{\alpha\beta}$ are calculated taking into account the contribution of internal degrees of freedom (inelastic collisions) as described in [10]. A degree of freedom is defined as a parameter corresponding to each independent variable necessary to describe the energy of a molecule [19]. A monoatomic molecule has three degrees of freedom corresponding to its translational energies in x, y and z directions. Polyatomic molecules have additional degrees of freedom corresponding to their rotational and vibrational

motions (see [20] for the analysis of degrees of freedom of CO_2 molecules). The total number of degrees of freedom in any molecule is equal to $3N_{\rm at}$ where $N_{\rm at}$ is the total number of atoms in a molecule [21]. It is assumed that air (approximated as nitrogen) has 2 internal degrees of freedom, while both hydrocarbons (n-dodecane and p-dipropylbenzene) have 20 internal degrees of freedom each. As shown in [10, 11], taking into account larger numbers of internal degrees of freedom does not affect the results.

As in [6, 8, 9, 11], the effects of the curvature of the droplet surface are ignored. This is justified by the fact that the thickness of the kinetic region is very small; in our case it is assumed equal to 10 mean free paths for n-dodecane molecules in saturated n-dodecane vapour at temperature equal to 600 K (ℓ).

Equations (15) are solved subject to the boundary conditions at the interface between the kinetic and liquid regions and at the interface between the kinetic and hydrodynamic regions (see Fig. 1). The first boundary condition for both components of the vapour can be presented as:

$$f_{vi\,(\rm out)} = \beta_i f_{vis} + (1-\beta_i) f_{vir}, \tag{17}$$

where f_{vis} is the distribution function of molecules leaving the liquid surface assuming that $\beta_i = 1$, f_{vir} is the distribution function of reflected molecules. Both f_{vis} and f_{vir} are assumed to be isotropic Maxwellian. The temperature for f_{vis} is assumed to be equal to T_s, while the temperature for f_{vir} is assumed to be equal to T_{Rd}. This is justified by the fact that the thickness of the kinetic region is small and the gas temperature just above the droplet surface is close to T_{Rd} [3]. At the boundary between the kinetic and hydrodynamic regions the distribution function of vapour components and air molecules entering the kinetic region is assumed to be Maxwellian, controlled by ρ_{Rd} for both components and T_{Rd}.

The contributions of both mass and heat transfer in the kinetic region are taken into account following the approach described in [11]. In [11] we took into account the dependence of the evaporation coefficient for n-dodecane on temperature as inferred from our molecular dynamics analysis [22]. Since no such analysis was performed for p-dipropylbenzene, we believe that it would be more consistent to assume that in both cases the evaporation coefficients for both components are equal to 1 at this stage.

The kinetic calculations were performed for pure n-dodecane droplets, and the following n-dodecane and p-dipropylbenzene molar fractions: 80% n-dodecane and 20% p-dipropylbenzene; 70% n-dodecane and 30% p-dipropylbenzene.

Chemical formulae, molar masses and molecular diameters of these vapour components and nitrogen (approximating air), used in our analysis, are given in Table 1.

Component	Chemical formula	Molar mass	Molecular diameter
n-dodecane	$C_{12}H_{26}$	170.3 kg/kmol	7.12 Å
p-dipropylbenzene	$C_{12}H_{18}$	162.27 kg/kmol	6.73 Å
nitrogen	N_2	28.97 kg/kmol	3.617 Å

Table 1

As in [11], the first step in the solution of Equations (15) is to perform an investigation of mass and heat transfer processes in the kinetic region for a set of values of ρ_{Rd} (for both vapour components) and T_{Rd}. We consider the problem of heating and evaporation of droplets in a hot gas (Diesel engine-like conditions) and these parameters are assumed to be in the ranges: $\rho_{Rd} < \rho_s$ and $T_{Rd} > T_s$. During the droplet heating process, the temperature increases away from the droplet; the evaporation process is possible when the vapour density decreases away from the droplet surface. For the chosen values of ρ_{Rd} and T_{Rd}, the solution to the Boltzmann Equations (15) in the kinetic region allows us to calculate the normalised mass and heat fluxes at the outer boundary of this region:

$$\tilde{j}_{\mathrm{k\,(n,p)}} = j_{\mathrm{k\,(n,p)}}/(\rho_0\sqrt{R_v T_0}), \qquad \tilde{q}_{\mathrm{k}} = q_{\mathrm{k}}/(p_0\sqrt{R_v T_0}),$$

where R_v is the gas constant referring to n-dodecane vapour, T_0 is the reference temperature chosen equal to 600 K, p_0 and ρ_0 are the saturated n-dodecane vapour pressure and density corresponding to T_0, ρ_0 is calculated from the ideal gas law, subscript $_{\mathrm{k}}$ stands for kinetic.

In [11] it was shown that for the case of heating and evaporation of n-dodecane droplets the values of $\tilde{q}_{\mathrm{k}}$ are almost independent of $\tilde{\rho}_{Rd} \equiv \rho_{Rd}/\rho_s$ in a certain range of $\tilde{\rho}_{Rd}$ and the values of $\tilde{j}_{\mathrm{k}}$ are almost do independent of $\tilde{T}_{Rd} \equiv T_{Rd}/T_s$ in a certain range of $\tilde{T}_{Rd}$ relevant to the conditions typical for Diesel engines. In what follows, it is demonstrated that this property is observed for the case of heating and evaporation of two-component (a mixture of n-dodecane and of p-dipropylbenzene) droplets.

Let us assume that molar fractions of n-dodecane and p-dipropylbenzene in the droplet are 80% and 20% respectively, droplet surface temperature is equal to 600 K, and $\tilde{\rho}_{Rd\,(n)} = \tilde{\rho}_{Rd\,(p)} \equiv \tilde{\rho}_{Rd}$. The plots of $\tilde{q}_{\rm k}$ versus $\tilde{\rho}_{Rd}$ for $\tilde{T}_{Rd} = 1.05$ and 1.1 are shown in Fig. 2. As one can see in this figure, the plots for these values of $\tilde{T}_{Rd}$ are the lines which are almost perfectly parallel to the $\tilde{\rho}_{Rd}$ axis. A similar conclusion was reached in the general case when $\tilde{\rho}_{Rd\,(n)} \neq \tilde{\rho}_{Rd\,(p)}$. The same result was obtained for the 70% n-dodecane and 30% p-dipropylbenzene mixture. This allows us to ignore the dependence of $\tilde{q}_{\rm k}$ on $\tilde{\rho}_{Rd}$ in agreement with the similar result obtained in [11].

The plots of mass fluxes of n-dodecane and p-dipropylbenzene predicted by the kinetic model ($\tilde{j}_{\rm k\,(n)}$ and $\tilde{j}_{\rm k\,(p)}$) versus $\tilde{T}_{Rd}$ for $\tilde{\rho}_{Rd} = 0.7$ for both components under the same conditions as in Fig. 2 are shown in Fig. 3. As one can see in this figure, the plots for these values of $\tilde{\rho}_{Rd}$ and in the range of $\tilde{T}_{Rd}$ shown, are the lines which are almost parallel to the $\tilde{T}_{Rd}$ axis. In contrast to the case shown in Fig. 2, a very weak dependence of j_k on $\tilde{T}_{Rd}$ can be observed, but this can be ignored in our analysis. A similar conclusion was reached in the general case when $\tilde{\rho}_{Rd\,(n)} \neq \tilde{\rho}_{Rd\,(p)}$. The same result was obtained for the 70% n-dodecane and 30% p-dipropylbenzene mixture. This allows us to ignore the dependence of $\tilde{j}_{\rm k}$ on $\tilde{T}_{Rd}$. Thus the results shown in Figs. 2 and 3 allow us to decouple the analysis of heat and mass fluxes in the kinetic region for $\tilde{\rho}_{Rd}$ in the range (0.7 – 1) and $\tilde{T}_{Rd}$ in the range (1 – 1.1).

The values of $\tilde{T}_{Rd}$ for two-component droplets were obtained following the same procedure as described in [11] for monocomponent droplets. This procedure is illustrated in Fig. 4 for an 80% n-dodecane and 20% p-dipropylbenzene droplet of radius 5 μm, surface temperature 600 K and gas temperature 1000 K. The value of $\tilde{\rho}_{Rd}$ was taken equal to 0.7. Recalling Fig. 2, we expect the results not to depend on the actual values of $\tilde{\rho}_{Rd}$. The plots of the heat flux predicted by the kinetic model, $\tilde{q}_{\rm k}$, versus $\tilde{T}_{Rd}$, and the heat flux in the hydrodynamic region predicted by the hydrodynamic model, $\tilde{q}_{\rm h} = q_{\rm h}/(p_0\sqrt{R_v T_0})$, versus $\tilde{T}_{Rd}$ (horizontal line), for these values of parameters are shown in Fig. 4. The intersection between the horizontal and inclined lines gives the required value of $\tilde{T}_{Rd} = 1.022$.

The plots of the mass flux predicted by the kinetic model, $\tilde{j}_{\rm k}$, versus $\tilde{\rho}_{Rd}$ for $\tilde{T}_{Rd} = 1.05$ (as follows from the analysis based on Fig. 3, the result is not expected to depend of $\tilde{T}_{Rd}$) and the mass flux predicted by the hydrodynamic model, $\tilde{j}_{\rm h} = j_{\rm h}/(\rho_0\sqrt{R_v T_0})$, for n-dodecane ($\tilde{j}_{\rm k\,(n)}$ and $\tilde{j}_{\rm h\,(n)}$) and p-dipropylbenzene ($\tilde{j}_{\rm k\,(p)}$ and $\tilde{j}_{\rm h\,(p)}$) versus $\tilde{\rho}_{Rd}$ ($\tilde{\rho}_{Rd\,(n)}$ or $\tilde{\rho}_{Rd\,(p)}$) are shown

in Fig. 5. The mass fluxes predicted by the hydrodynamic model are shown by the horizontal lines. This figure is presented for the same parameters as in Fig. 4. Following [11], it was assumed that ρ_{Rd} in Equation (14) can be replaced with ρ_s. The intersections between the horizontal and inclined lines give the required values of $\tilde{\rho}_{Rd}$: $\tilde{\rho}_{Rd(n)} = 0.983$ for n-dodecane and $\tilde{\rho}_{Rd(p)} = 0.987$ for p-dipropylbenzene. Similar values of $\tilde{T}_{Rd}$ and $\tilde{\rho}_{Rd}$ were obtained for other values of T_g, T_s and R_d relevant for Diesel engine conditions ($T_g = 750$ K, $T_g = 700$ K; for values of T_s in the range 300 K to temperatures close to the critical temperature, and the range of molar fractions of n-dodecane and p-dipropylbenzene predicted by hydrodynamic calculations). The corresponding values of $\tilde{T}_{Rd}$ and $\tilde{\rho}_{Rd}$ were used for the analysis of heating and evaporation of mono- and two-components droplets in realistic Diesel engine-like conditions.

Following the above procedure, a set of values of $\tilde{\rho}_{Rd}$ and $\tilde{T}_{Rd}$ were obtained for a number of specific pairs of values of droplet surface temperatures and radii, predicted by the hydrodynamic model. Once the values of $\tilde{\rho}_{Rd}$ were obtained, then for kinetic modelling the values of ρ_s in Equation (8) were replaced by ρ_{Rd}. For the intermediate values of these parameters the values of $\tilde{\rho}_{Rd}$ and $\tilde{T}_{Rd}$ were interpolated. The thickness of the kinetic region is assumed to be infinitely small. Since $\rho_{Rd} < \rho_s$, then the value of B_M predicted by the kinetic model ($B_{M,\,k}$) is always less than the value of B_M predicted by the hydrodynamic model ($B_{M,\,h}$). Hence, we can expect that the evaporation rate predicted by the kinetic model is always less than the one predicted by the hydrodynamic model for the same droplet surface temperature.

The decrease in the values of B_M predicted by the kinetic model is expected to lead to a corresponding decrease in the values of B_T and ultimately the values of the convection heat transfer coefficient h. This will lead to a decrease in the values of T_{eff}. On the other hand, slowing down of the evaporation process, predicted by the kinetic model, will lead to a decrease in $|\dot{R}_d|$, and ultimately an increase in T_{eff}. The balance between these two processes will lead to either a decrease or an increase in the predicted droplet surface temperatures.

Note that we did not take into account the effect of changes in the droplet evaporation rates due to the changes in droplet surface temperatures predicted by the kinetic model, as in this case we would need to use the corrected values of j_{vi} for the mass fluxes predicted by the hydrodynamic model. This would lead to new values of $\tilde{\rho}_{Rd}$ and the new values of droplet surface

temperature etc. The investigation of this effect is beyond the scope of this paper.

In the next section, the results of modelling of specific droplets are demonstrated.

3. Results

The results of calculation of the radii and surface temperatures of a droplet with initial radius and temperature equal to 5 μm and 300 K, respectively, immersed into gas with temperature 1000 K are shown in Fig. 6. Three types of droplets have been considered: pure n-dodecane, a mixture of 80% n-dodecane and 20% p-dipropylbenzene, and a mixture of 70% n-dodecane and 30% p-dipropylbenzene (the contributions of components refer to their molar fractions; see Table 2). Results of both hydrodynamic and kinetic calculations are presented. In kinetic calculations both heat and mass transfer in the kinetic region and the effects of inelastic collisions are taken into account. The evaporation coefficient is assumed equal to 1 for both components.

Plots	Model	Molar fraction of n-dodecane	Molar fraction of p-dipropylbenzene
1	Kinetic	100%	0%
2	Kinetic	80%	20%
3	Kinetic	70%	30%
4	Hydrodynamic	100%	0%
5	Hydrodynamic	80%	20%
6	Hydrodynamic	70%	30%

Table 2

Since the values of ρ_{Rd} were estimated as perturbations of ρ_s predicted by the hydrodynamic model, the calculations of the droplet radii predicted by the kinetic model had to be terminated before the evaporation time predicted by the hydrodynamic model (which is always less than the evaporation time predicted by the kinetic model). Then the values of the droplet radii predicted by the kinetic model were extrapolated until the complete evaporation of the droplet.

As one can see from Fig. 6, both the addition of p-dipropylbenzene and kinetic effects lead to an increase in the evaporation time of droplets. To estimate the effect of droplet composition on the kinetic effects, the following error function is introduced:

$$E \equiv \frac{t_{e(k)} - t_{e(h)}}{t_{e(k)}} \times 100\%, \tag{18}$$

where $t_{e(k\,(h))}$ is the evaporation time predicted by the kinetic (hydrodynamic) models. E is estimated as a percentage. Note that $t_{e(k)} > t_{e(h)}$. The values of E for the three mixtures presented in Fig. 6 are the following: 100% n-dodecane – $E = 1.61\%$, 80% n-dodecane – $E = 1.70\%$, 70% n-dodecane – $E = 2.5\%$. Thus, the values of E increase with increasing p-dipropylbenzene contribution. In all cases, these values remain less than 3%, and they need to be taken into account only in the case of very accurate modelling of this process.

The same plots as in Fig. 6 but for gas temperature equal to 700 K are shown in Fig. 7. Comparing Figs. 6 and 7 one can see that the decrease in gas temperature from 1000 K to 700 K leads to more that doubling of the evaporation time and reduction of the kinetic effects for all three mixtures. For 100% n-dodecane – $E = 0.22\%$, 80% n-dodecane – $E = 0.32\%$, 70% n-dodecane – $E = 0.58\%$. As in the case of gas temperature equal to 1000 K, the values of E increase with increasing p-dipropylbenzene contribution. These errors can be safely ignored in all feasible applications.

We can expect that the kinetic effects will become even more noticeable at temperatures greater than 1000 K. In this case, however, the droplet surface temperatures are expected to approach the critical temperature well before its final evaporation. Our model is expected to be less reliable as it is based on the assumption that droplet surface temperature is not close to the critical temperature.

The main problem with approximation of Diesel fuel by a mixture of n-dodecane and p-dipropylbenzene is that the accuracy of this approximation for modelling droplet heating and evaporation has not yet been carefully investigated for a wide range of available Diesel fuels. In the case of Diesel fuel considered in [11], the evaporation time of droplets with initial radii 5 μm in gas at temperature 700 K, predicted by this approximation, turned out to be about one half of the evaporation time predicted for a Diesel fuel droplet in these conditions, although the prediction of this approximation is better than the one for a pure n-dodecane droplet. As shown in [14], a reasonably

accurate approximation for both the evaporation time and time evolution of droplet surface temperature can be achieved when Diesel fuel is approximated by about 15 quasi-components/components. Of course, it is not possible to perform kinetic modelling for such a mixture; the approximation of Diesel fuel by a two-component mixture is bound to be crude, although nobody, to the best of our knowledge, has attempted to investigate this problem in depth and found an optimal two-component approximation of Diesel fuel (apart from the approximation used in this paper). We were able to show that the mixture 10% n-dodecane and 90% dodecylbenzene ($C_{18}H_{30}$) leads to the prediction of droplet evaporation times close to the one predicted for a Diesel fuel droplet. To achieve this, however, it was necessary to tolerate rather large differences in the predicted surface temperatures for this approximation and for the approximation of Diesel fuel considered in [14].

4. Conclusions

The previously developed kinetic model for two-component droplet heating and evaporation into a high pressure background gas (air) has been applied to the analysis of n-dodecane and p-dipropylbenzene mixture droplet heating and evaporation in Diesel engine-like conditions. As in our previous papers (e.g. [11]), the kinetic heating and evaporation model is based on the introduction of the kinetic region in the immediate vicinity of the heated and evaporating droplets, where the dynamics of molecules are described in terms of the Boltzmann equations for vapour components and air, and the hydrodynamic region. In contrast to [11], the presence of two components in the vapour are taken into account. The boundary conditions at the outer boundary of the kinetic region are introduced by matching the mass fluxes of vapour components leaving the kinetic region and entering into the surrounding hydrodynamic region. The effects of finite thermal conductivity inside the droplets and inelastic collisions in the kinetic region are taken into account as in [11]. In contrast to [11], we also considered the effects of species diffusivity inside the droplets. The evaporation coefficient for both components is assumed equal to 1.

It is pointed out that for the parameters typical for Diesel engine-like conditions, the heat flux in the kinetic region is a linear function of the vapour temperature at the outer boundary of this region, but is almost independent of the densities of vapour components at this boundary in a certain range of these densities, as in the case of monocomponent droplets (see [11]). The

mass fluxes of both components in the kinetic region are shown to decrease almost linearly as their densities at the outer boundary of the kinetic region increase, but are almost independent of the temperatures at this boundary in a certain range of these temperatures, as in the case of monocomponent droplets. Using the matching conditions at the outer boundary of the kinetic region, the values of temperature and densities of both components at this boundary have been found.

The model is tested for the analysis of heating and evaporation of droplets with initial radii and temperature equal to 5 μm and 300 K, immersed into gas with temperatures 1000 K and 700 K for three droplet compositions (in terms of molar fractions): pure n-dodecane, a mixture of 80% n-dodecane and 20% p-dipropylbenzene, and a mixture of 70% n-dodecane and 30% p-dipropylbenzene. It is shown that both the addition of p-dipropylbenzene and kinetic effects lead to an increase in the evaporation time of droplets. In all cases, the kinetic effects on the droplet evaporation times increase with increasing p-dipropylbenzene contribution and gas temperature.

Acknowledgements

The authors are grateful to EPSRC (UK) (Project EP/J006793/1), INTERREG IVa (Project E3C3, Reference 4274) and the Russian Foundation for Basic Research (Grant 14-08-00467) for their financial support of this project.

References

[1] U. Fritsching, Spray Simulation. Cambridge: Cambridge University Press (2004).

[2] E.E. Michaelides, Particles, Bubbles & Drops. New Jersey: World Scientific (2006).

[3] N.A. Fuchs, Evaporation and Droplet Growth in Gaseous Media. London: Pergamon Press (1959).

[4] S.S. Sazhin, Advanced models of fuel droplet heating and evaporation, Prog. in Energy Combustion Sci. 32 (2006) 162-214.

[5] S.S. Sazhin, Droplets and Sprays. Springer (2014).

[6] A.P. Kryukov, V.Yu. Levashov, S.S. Sazhin, Evaporation of Diesel fuel droplets: kinetic versus hydrodynamic models, Int. J. Heat Mass Transfer 47 (2004) 2541-2549.

[7] I.N. Shishkova, S.S. Sazhin, A numerical algorithm for kinetic modelling of evaporation processes, J. Computational Physics 218 (2006) 635-653.

[8] S.S. Sazhin, I.N. Shishkova, A.P. Kryukov, V.Yu. Levashov, M.R. Heikal, Evaporation of droplets into a background gas: kinetic modelling, Int. J. Heat Mass Transfer 50 (2007) 2675-2691.

[9] S.S. Sazhin, I.N. Shishkova, A kinetic algorithm for modelling the droplet evaporation process in the presence of heat flux and background gas, Atomization and Sprays 19 (2009) 473-489.

[10] I.N. Shishkova, S.S. Sazhin, J.-F. Xie, A solution of the Boltzmann equation in the presence of inelastic collisions, J. Computational Physics 232 (2013) 87-99.

[11] S.S. Sazhin, J.-F Xie, I.N. Shishkova, A.E. Elwardany, M.R. Heikal, A kinetic model of droplet heating and evaporation: effects of inelastic collisions and a non-unity evaporation coefficient, Int. J. Heat and Mass Transfer 56 (2013) 525-537.

[12] C. Ledier, M. Orain, F. Grisch, J. Kashdan, G. Bruneaux, Vapour concentration measurements in biofuel sprays using innovative Planar Laser-Induced Fluorescence strategies. Proceedings of ILASS Europe 2011, 24th European Conference on Liquid Atomization and Spray Systems, Estoril, Portugal, September 2011 (Book of Abstracts, page 100; full paper is on the conference CD).

[13] V.M. Gun'ko, R. Nasiri, S.S. Sazhin, F. Lemoine, F. Grisch, A quantum chemical study of the processes during the evaporation of real-life Diesel fuel droplets, Fluid Phase Equilibria, 356 (2013) 146156.

[14] S.S. Sazhin, M. Al Qubeissi, R. Nasiri, V.M. Gunko, A.E. Elwardany, F. Lemoine, F., Grisch, M.R. Heikal, A multi-dimensional quasi-discrete model for the analysis of Diesel fuel droplet heating and evaporation, Fuel 129 (2004) 238-266.

[15] Agency for Toxic Substances and Disease Registry (ATSDR). Toxicological profile for fuel oils. Atlanta, GA: U.S. Department of Health and Human Services, Public Health Service, 1995.

[16] V.M. Gun'ko, R. Nasiri, S.S. Sazhin, A study of the evaporation and condensation of n-alkane clusters and nanodroplets using quantum chemical methods, Fluid Phase Equilibria 366 (2014) 99-107.

[17] I.N. Shishkova, S.S. Sazhin, A solution of the Boltzmann equation in the presence of three components and inelastic collisions, Int. J. Heat and Mass Transfer 71 (2014) 26-34.

[18] B. Abramzon, S.S. Sazhin, Convective vaporization of fuel droplets with thermal radiation absorption, Fuel 85 (2006) 32-46.

[19] W.P. Crummet, A.B. Western, University Physics. Dubuque (USA), Wm. C. Brown Publishers (1994).

[20] S.S. Sazhin, P. Wild, C. Leys, D. Toebaert, E.M. Sazhina, The three temperature model for the fast-axial-flow CO_2 laser, J Physics D: Applied Physics 26 (1993) 1872-1883.

[21] P. Atkins, J. de Paula, Atkin's Physical Chemistry (Seventh Edition), Oxford: Oxford University Press (2002).

[22] J.-F. Xie, S.S. Sazhin, B.-Y. Cao, Molecular dynamics study of the processes in the vicinity of the n-dodecane vapour/liquid interface, Phys. Fluids 23 (2011) 112104.

Figure Captions

Fig. 1 Liquid, kinetic and hydrodynamic regions near the surface of the droplet. T_s is the droplet surface temperature, $\rho_{s\,(n,p)}$ are the n-dodecane $(_n)$ and p-dipropylbenzene $(_p)$ vapour densities in the immediate vicinity of the droplet surface, T_{Rd} and $\rho_{Rd\,(n,p)}$ are the temperature and the n-dodecane $(_n)$ and p-dipropylbenzene $(_p)$ vapour densities at the outer boundary of the kinetic region.

Fig. 2 The plots of normalised heat flux $\tilde{q}_{\rm k}$ versus $\tilde{\rho}_{Rd}$ for $\tilde{T}_{Rd} = 1.05$ and $\tilde{T}_{Rd} = 1.10$ for an 80% n-dodecane and 20% p-dipropylbenzene mixture at droplet surface temperature 600 K.

Fig. 3 The plots of mass fluxes, predicted by the kinetic model, of n-dodecane $\tilde{j}_{\rm k\,(n)}$ and p-dipropylbenzene $\tilde{j}_{\rm k\,(p)}$ versus $\tilde{T}_{Rd}$ for $\tilde{\rho}_{Rd} = 0.7$ under the same conditions as in Fig. 2.

Fig. 4 The plots of the heat flux predicted by the kinetic model, $\tilde{q}_{\rm k}$, versus $\tilde{T}_{Rd}$ and the heat flux predicted by the hydrodynamic model, $\tilde{q}_{\rm h} = q_{\rm h}/(p_0\sqrt{R_v T_0})$, versus $\tilde{T}_{Rd}$ (horizontal line) for $\tilde{\rho}_{Rd} = 0.7$ and an 80% n-dodecane and 20% p-dipropylbenzene mixture droplet of radius 5 μm, surface temperature 600 K and gas temperature 1000 K. The intersection between the $\tilde{q}_{\rm k}$ and $\tilde{q}_{\rm h}$ gives the value of $\tilde{T}_{Rd} = 1.022$.

Fig. 5 The plots of the mass flux of the components predicted by the kinetic model, $\tilde{j}_{\rm k}$, versus $\tilde{\rho}_{Rd}$ for $\tilde{T}_{Rd} = 1.05$ and the hydrodynamic model, $\tilde{j}_{\rm h} = j_{\rm h}/(p_0\sqrt{R_v T_0})$, for n-dodecane $(\tilde{j}_{\rm h\,(n)})$ and p-dipropylbenzene $(\tilde{j}_{\rm h\,(p)})$ versus $\tilde{\rho}_{Rd}$ ($\tilde{\rho}_{Rd\,(n)}$ and $\tilde{\rho}_{Rd\,(p)}$ for the same parameters as in Fig. 4). $\tilde{j}_{\rm h\,(n)}$ and $\tilde{j}_{\rm h\,(p)}$ are shown by horizontal lines. The intersections between the horizontal and inclined lines give the required values of $\tilde{\rho}_{Rd}$: $\tilde{\rho}_{Rd(n)} = 0.983$ for n-dodecane and $\tilde{\rho}_{Rd(p)} = 0.987$ for p-dipropylbenzene.

Fig. 6 The plots of R_d and T_s versus time, as predicted by the kinetic and hydrodynamic models for droplets with initial radii and temperature equal to 5 μm and 300 K, immersed into gas with temperature 1000 K; pure n-dodecane and mixtures of n-dodecane and p-dipropylbenzene have been considered; the link between the modelling conditions and the plots is shown

in Table 2. **A** refers to the zoomed part of the figure for droplet surface temperatures; **B** refers to the zoomed part of the figure for droplet radii.

Fig. 7 The same as Fig. 6, but for the gas temperature 700 K.

Table Captions

Table 1 Chemical formulae, molar masses and molecular diameters of n-dodecane, p-dipropylbenzene and nitrogen, used in our analysis.

Table 2 The link between the modelling conditions and the plots shown in Figs. 6 and 7.

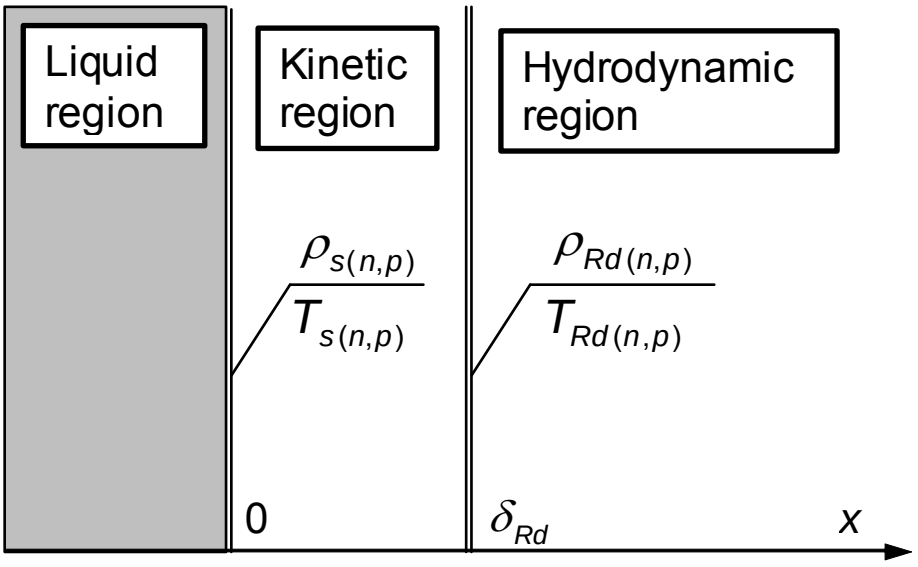
Liquid region
Kinetic region
Hydrodynamic region
$\rho_{s(n,p)}$
$T_{s(n,p)}$
$\rho_{Rd(n,p)}$
$T_{Rd(n,p)}$
0
δ_{Rd}
x

Fig.1.

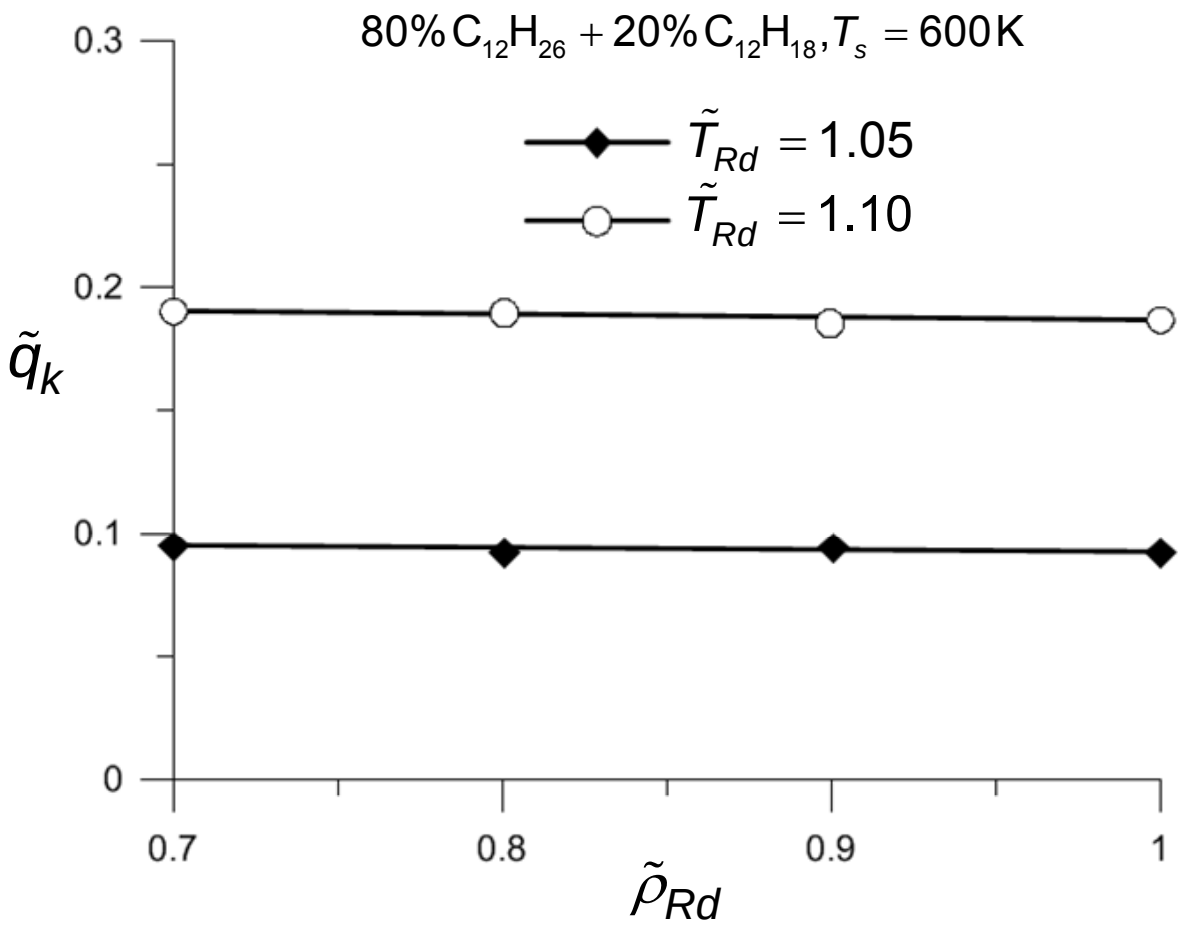
80% C12H26 + 20% C12H18, Ts = 600 K
T̃Rd = 1.05
T̃Rd = 1.10
q̃k
0.3
0.2
0.1
0
0.7
0.8
0.9
1
ρ̃Rd

Fig. 2

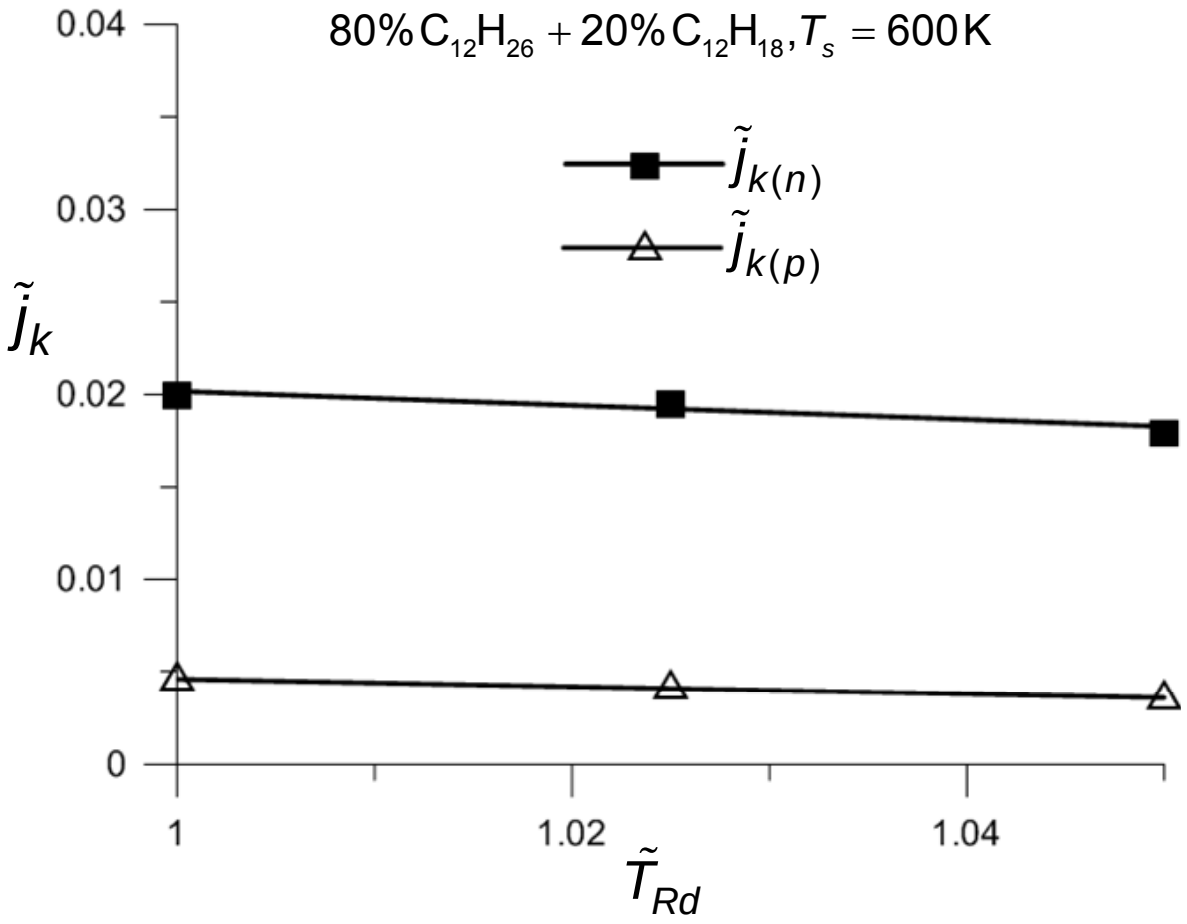
80% C12H26 + 20% C12H18, Ts = 600 K
0.04
0.03
0.02
0.01
0
j̃k
j̃k(n)
j̃k(p)
1
1.02
1.04
T̃Rd

Fig. 3

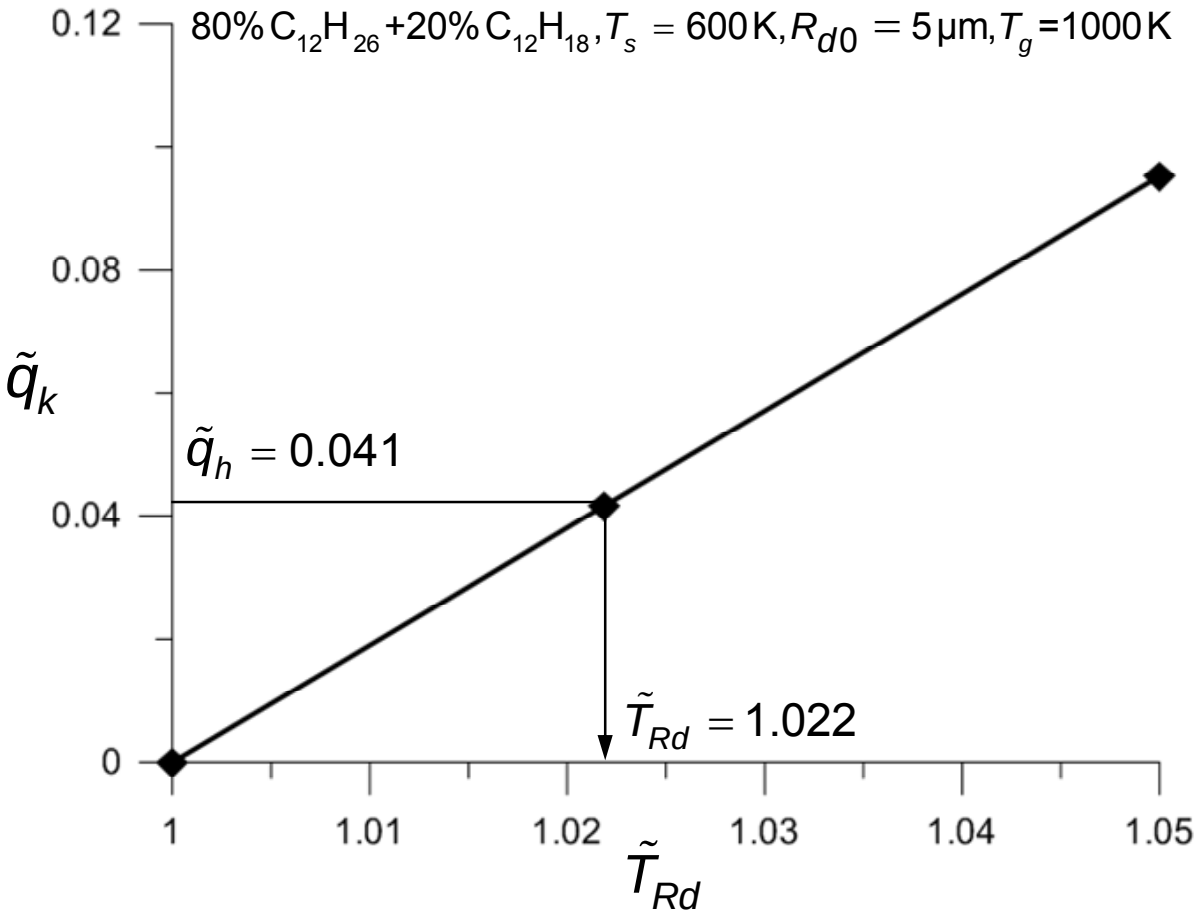
80% C12H26 +20% C12H18, Ts = 600 K, Rd0 = 5 μm, Tg =1000 K
0.12
0.08
0.04
0
q̃k
q̃h = 0.041
T̃Rd = 1.022
1
1.01
1.02
1.03
1.04
1.05
T̃Rd

Fig. 4

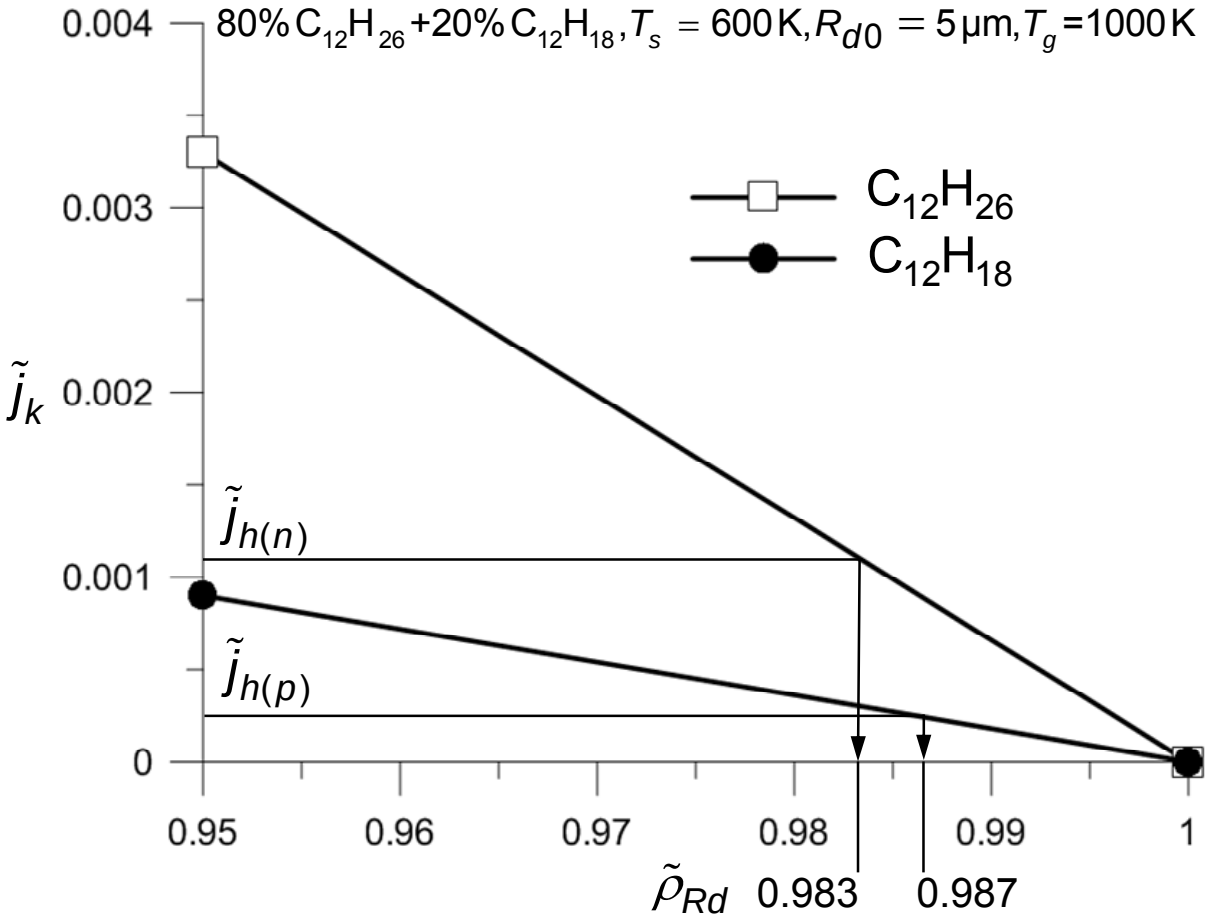
80% C12H26 +20% C12H18, Ts = 600 K, Rd0 = 5 μm, Tg =1000 K
0.004
0.003
0.002
0.001
0
j̃k
C12H26
C12H18
j̃h(n)
j̃h(p)
0.95
0.96
0.97
0.98
0.99
1
ρ̃Rd
0.983
0.987

Fig. 5

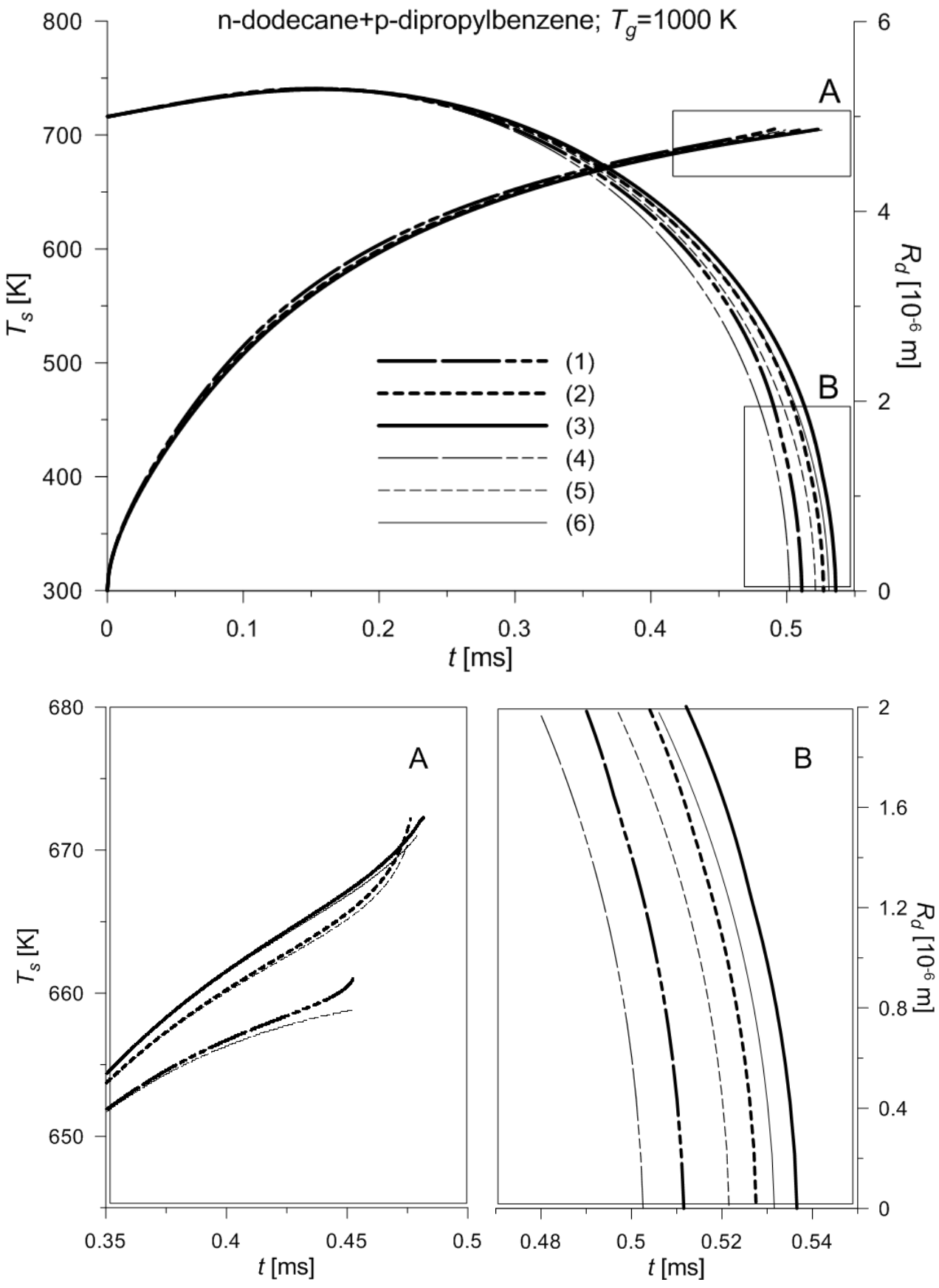
n-dodecane+p-dipropylbenzene; T_g=1000 K
T_s [K]
R_d [10^{-6} m]
t [ms]
A
B
(1)
(2)
(3)
(4)
(5)
(6)

Fig.6

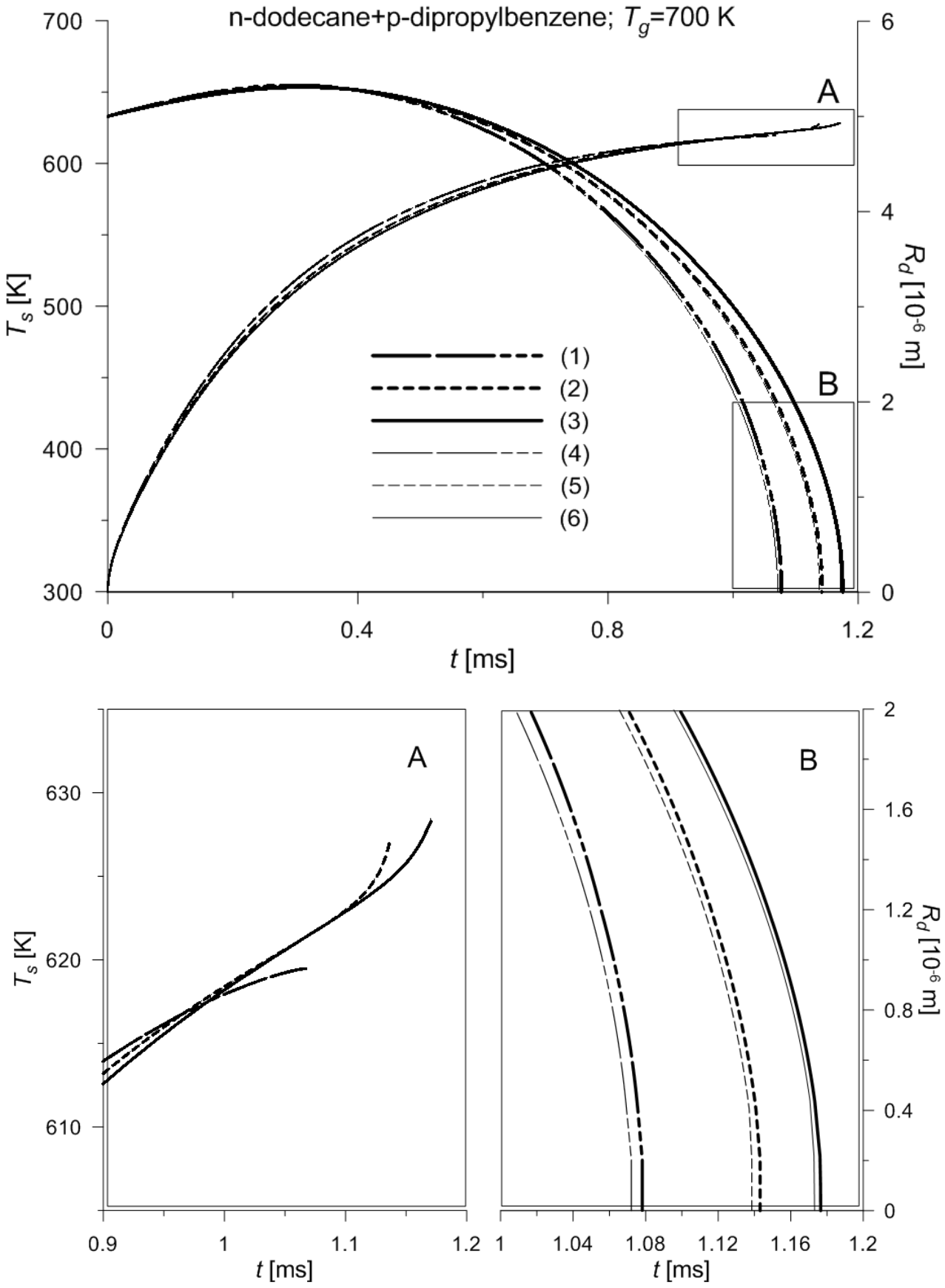
n-dodecane+p-dipropylbenzene; T_g=700 K
T_s [K]
R_d [10^{-6} m]
t [ms]
(1)
(2)
(3)
(4)
(5)
(6)
A
B

Fig.7